The Effects of Armour Fit and Body Habitus on Behind Armour Blunt Trauma Loading

A. Iwaskiw[1], K. Ott[1], N. Hahne[1], M. Vignos[1], N. Steiner[1], R. Hingorani[1], M. Clark[2]

[1]*The Johns Hopkins University Applied Physics Laboratory (JHU/APL), 11100 Johns Hopkins Road, Laurel, MD 20723, alexander.iwaskiw@jhuapl.edu*
[2] *U.S. Special Operations Command, 10 General Greene Avenue, Natick, MA 01760*

Abstract. Injury due to behind armour blunt trauma (BABT) is a concern to the warfighter. An existing hypothesis related to BABT is that the distance between the backface of the armour and the wearer, as well as the physical anatomical composition of the impact site, could influence BABT risk. This study utilised two separate experiments, one measuring impact force and the other measuring clay deformation to investigate this hypothesis. Live ammunition impacted hard armour plates backed by air, flesh, and either clay or a load cell system. Flesh was excised from the torso of untested postmortem human surrogates (PMHS). Sixteen load cell backed non-penetrating ballistic tests, measuring peak force and impulse, were conducted across various flesh thicknesses (0-20 mm), air gaps (0-25 mm) and velocities. In addition, 15 clay backed tests, with similar air gap and flesh thickness conditions, were tested evaluating depth left in clay. After the tests, the results were fit with models that developed a relationship between striking velocity, air gap, flesh thickness and the loading metrics of interest. Air gap and flesh thickness were found to be protective, where loading decreased with increased air gap and flesh thickness. Measured force had a decaying exponential relationship with these parameters, whereas clay deformation had a decaying linear relationship. To verify the relationship developed in these experiments, loading conditions were predicted using fit and body habitus variables measured in a separate study where BABT injuries were induced in full PMHS models. The estimated loading conditions, when using specific air gaps and flesh thicknesses, were better predictors of injury than using striking velocity alone in these experiments. This supports the hypothesis that flesh and air gap contribute to reducing the loading on the anatomy and should be considered when assessing risk of BABT.

1. INTRODUCTION

Behind armour blunt trauma (BABT) occurs when the backface of ballistic armour strikes the wearer without full penetration of the projectile, and such injuries are a concern for warfighters. [1]. The mechanics of BABT events are characterised by high rate and focal loading. When this type of event is centred over the sternum, it can result in injuries ranging from skin lacerations and abrasions to rib fractures and organ damage [2]. While historically rare, recent conflicts involving advanced personal armour systems have led to documented BABT cases [3]. These cases have confirmed the types of injuries seen in biomechanical models used to study BABT and emphasised the need to further understand BABT effects.

Military body armour optimization would benefit through development of injury-based standards. Current standards utilise a clay backing to both mimic the presence of tissue as well as provide a metric, i.e. permanent deformation, for understanding injury risk [4]. However, there have been many limitations observed in literature of this standard driving the need for a more accurate metric [5], [6]. In response, the past two decades have seen numerous efforts to refine injury risk assessment beyond clay testing. Recent studies involving postmortem human surrogates (PMHS) and animal models use various BABT loads to induce and study BABT injuries experimentally [2], [7], [8], [9], [10]. Simulated BABT injuries enable the development of continuous injury risk models using approaches such as logistic regression and survival analysis. However, significant uncertainty exists in these models, likely due to variability in biological models, which can manifest in multiple ways [11]. In studies using PMHS, biological factors such as age, height, and weight can be controlled through exclusion criteria to reduce variation. However, other factors that cannot always be screened or controlled may influence BABT loading. One such factor is body habitus—the overall physical build and shape of an individual—which can affect both armour plate fit (including the air gap between the armour backface and the wearer) and the amount of soft tissue between the armour backface and the skeleton [12], [13].

Body habitus has been recognised as a key variable in injury risk assessment across various fields. In automotive injury biomechanics, its effects have been extensively studied, with more recent research focusing on its role in blunt injury risk [14], [15], [16], [17]. In BABT research, the velocity of the armour backface is known to decrease rapidly within the first few centimetres, suggesting that the gap between the armour and the body could significantly reduce the force transmitted to the wearer [18], [19]. Body habitus is hypothesised to influence injury risk by altering armour fit and modifying

https://doi.org/10.52202/081621-0008

anatomical composition at the point of impact. This study aims to investigate its effects on BABT loading correlates (force response and clay deformation) by varying air gap distance and flesh thickness through isolated load cell and clay testing. These laboratory findings are then compared with injury outcomes from prior PMHS BABT tests to assess the influence of air gap and flesh thickness on BABT outcomes.

2. METHODS

2.1 Armour and threat

The same projectile and armour combination was used for all tests in this study. The projectile chosen was the 7.62 x 51 mm M80 Ball, while the striking velocity, flesh thickness and standoff ranges were all derived from previously conducted PMHS tests [2]. The armour used for this study was the same as armour used during the PMHS tests, namely an ultra-high molecular weight polyethylene (UHMWPE) composite multi-curved plate with a Small Arms Protective Insert (SAPI) cut geometry. As with the previous PMHS studies, each plate was shot once at a location over the centre of the load cell. The plates utilised in this study did not have a soft armour backing behind the hard armour plate as these plates were designed to be stand alone.

2.2 General test setup

To examine the effect of body habitus and specifically flesh thickness, excised tissue from PMHS were placed in a custom fixture over the load cell or clay block and positioned between the armour plate and backing material. A diagram of the setup can be found in Figure 1. As indicated in the setup, an approximate square section of PMHS flesh, 300 mm x 300 mm, was excised from PMHS across the anterior thorax and abdominal region. The PMHS flesh components used for this harvesting were all male, fresh frozen specimen procured under institutional review board exemption approval through Johns Hopkins Medical Institutions and were all untested prior to flesh harvesting. Custom fixtures were used to position the flesh sample and trim the tissue thickness to the targeted value. When the flesh was excised, an initial measurement was taken using callipers at the impact site, to determine which thickness range was closest to minimize the amount of flesh trimmed for each sample. After trimming, final calliper measurements were made at the impact site and were used as the main flesh thickness parameters to be analysed in the study.

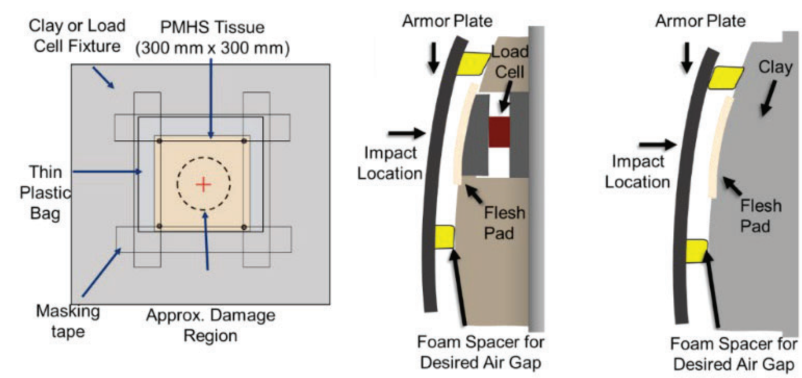

Figure 1. Diagram of tissue placement over backing fixture from a front on view (left), sagittal view of the load cell test setup (middle) and the clay setup (right).

The other variable that was controlled for was the air gap between the armour plate and the backing material. This distance was representative of the offset that an armour plate might naturally sit at due to the different body habitus of individuals. In order to both achieve the desired air gap while also approximating the material response of the structures that were driving this air gap to occur, open cell urethane foam of different thicknesses was used to achieve two different standoff positions. These spacers were placed above and below the impact location to ensure a uniform offset from the load cell and clay block. A FARO (FARO Technologies Lake Mary, Florida) coordinate measurement machine was used to determine the air gap by digitizing a point on the backing material, donning the amour, then digitizing a point on the surface of the armour. The thickness of the armour was then subtracted from

https://doi.org/10.52202/081621-0008

the measurement, resulting in an air gap measurement at the impact site along the direction of the ballistic trajectory.

2.3 Load cell test setup

Prior to testing, a custom 3D printed fixture (glass filled nylon) was created and was rigidly mounted to a 55 cm x 55 cm steel plate to provide a fixed boundary condition. The geometry of the 3D printed portion was designed to have the same curvature as the plate used for testing, with an obliquity of approximately 6 degrees at the site of impact. Within the contoured mounting fixture, a single piezo-electric load cell (PCB Model 200C50, range capacity of 222.4 kN) with a 152.4 mm diameter 4140 steel alloy impact cap was used. The impact cap was contoured to follow the curvature of the backface of the armour geometry as well. The fixture and setup can be seen in Figure 2. A total of 16 load cell backed tests were conducted.

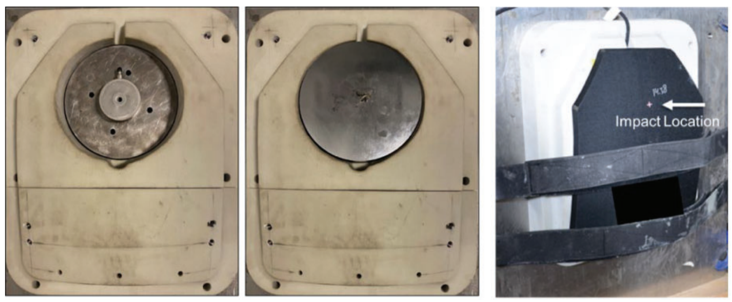

Figure 2. View of load cell fixture without cap (left), with 152.4 mm diameter impact cap (middle) and view of armour on fixture before test (right).

2.4 Clay test setup

Clay ballistic testing generally followed the clay calibration methods described in NIJ 0101.03 [5]. The armour was placed on a conditioned and tempered clay block, with a hand rolled template used to ensure no air gaps behind the curved armour plate. The clay was scanned before and after each test using a FARO laser scanner to create a point cloud representation of the clay surface. Geomagic Studio software (3D Systems, Rock Hill, South Carolina) was used to transform the point cloud into a surface model and calculate the clay deformation geometry (i.e., deformation left in clay). This resulting clay deformation value is termed adjusted backface deformation (BFD) due to the fact that air gap and flesh thickness were included in the test setup resulting in the armour not being pressed up directly to the clay. This value should not be used as a backface signature value (BFS) as it has different setup conditions, but it can be used in relative comparisons. A total of 15 clay backed tests were conducted.

2.5 Test matrix

All tests were conducted at an NIJ certified ballistic laboratory (Element U.S. Space & Defence, Belcamp, MD). Pre-test, the armour plate was placed in position, using elastic straps, over the backing material and fixture with the resulting air gap collected using a FARO arm. Data from the load cell was collected using a high-rate data acquisition system (Dewetron Inc., East Greenwich, RI, model DEWE-801) at a 1 MHz sampling rate. Three striking velocities (600, 762 and 915 m/s), three different flesh thickness values (0, 5-10 and 15-20 mm) and three different air gaps (0, 12 and 25 mm) were targeted. Table 1 shows the test matrix used for this study with the achieved striking velocities, tissue thickness, and achieved air gap.

Table 1. Experimental Test Matrix

Test #	Backing Condition	Striking Velocity (m/s)	Air Gap (mm)	Tissue Thickness (mm)
1	Load Cell	606	12.5	0
2	Load Cell	611	25.1	0
3	Load Cell	595	12.2	8.8
4	Load Cell	612	27.9	10.3
5	Load Cell	605	0	17.5
6	Load Cell	612	1.3	18.6
7	Load Cell	763	24.5	0
8	Load Cell	764	1.6	6.4
9	Load Cell	763	14.8	8.8
10	Load Cell	765	23	9.6
11	Load Cell	765	14.5	18.3
12	Load Cell	918	11.9	0
13	Load Cell	908	26.1	6.4
14	Load Cell	928	14.2	8
15	Load Cell	914	25.1	11.8
16	Load Cell	907	3.2	10

Test #	Backing Condition	Striking Velocity (m/s)	Air Gap (mm)	Tissue Thickness (mm)
17	Clay	604	11.4	0
18	Clay	606	24.3	0
19	Clay	594	12	4.8
20	Clay	604	23.6	7.1
21	Clay	612	4.3	12.9
22	Clay	611	0	17
23	Clay	611	0	22.7
24	Clay	758	28.3	0
25	Clay	758	3.1	7.5
26	Clay	760	12.1	8.5
27	Clay	763	23.6	2.8
28	Clay	760	9.9	11.8
29	Clay	759	0	0
30	Clay	926	0	0
31	Clay	926	10	0

3. RESULTS

3.1 Load cell results and parametric model

Representative traces for two tests demonstrating the effects of each of the variables examined in this study are found in Figure 3. Each test exhibited similar bi-modal responses with a large initial peak followed by a generally smaller secondary peak. The response decays rapidly after this initial response, oscillating around 0 N within 0.5 ms. As expected, the force measured at the load cell decreased with lower striking velocities. Similarly, increasing the air gap or flesh thickness led to a reduction in recorded force. However, variations in air gap had a more pronounced effect on force response compared to changes in flesh thickness.

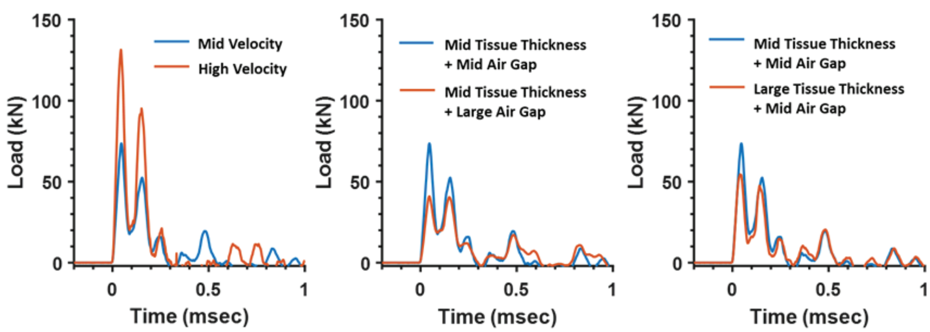

Figure 3. Force-time curves for two different ballistic tests varying the velocity (left), air gap (middle) and flesh thickness (right) while keeping the other two variables constant

Since the force response was similar across the different tests, the initial peak force was selected as a potential metric to correlate to injury. This initial peak primary force response was investigated as a function of air gap and flesh thickness as shown in Figure 4 for each of the striking velocities tested. As seen in the peak response, there was an implied correlation between air gap and the initial peak force response with less of a clear relationship between this peak force response and the flesh thickness.

https://doi.org/10.52202/081621-0008

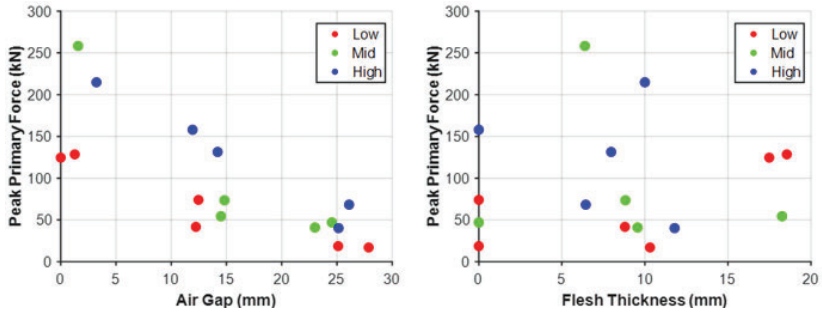

Figure 4. Initial peak force values as a function of air gap (left) and flesh thickness (right) with the three striking velocities represented by the red, green and blue dots

These results implied that the force response could be modelled using an exponential decaying model. This proposed relationship is shown in equation 1 where the peak primary force is a function of the striking velocity, air gap and tissue thickness. The model was fit by using a standard least squares fit between the natural log of peak force versus striking velocity, air gap and tissue thickness. The fit coefficient values were calculated using JMP Pro (Version 17.0.0, JMP Statistical Discovery LLC, Cary, NC). These resulting coefficient values and their associated p-values are shown in Table 2. These parameters resulted in a model that was able to predict actual peak force values with an R^2 value of 0.95.

$$\text{Peak Primary Force (kN)} = e^{b_0+b_1*Striking\ Vel.\ (m/s)+b_2*Air\ Gap\ (mm)+b_3*Tissue\ Thick.\ (mm)} \quad (1)$$

Table 2. Coefficients calculated for the exponential decaying model fit (equation 1)

Term	Coefficient Estimate	P value
Intercept	3.33	<0.0001
Striking Velocity (m/s)	0.003	<0.0001
Air Gap (mm)	-0.078	<0.0001
Tissue Thickness (mm)	-0.021	0.0345

3.2 Clay results and parametric model

In addition to tests conducted over load cells, the same test series was conducted over clay blocks with flesh and air gaps incorporated. Since clay BFS is used in the evaluation of the effectiveness of armour systems, it was important to see how this metric would be affected by the presence of standoff and flesh thickness. An evaluation of the adjusted clay BFD as a function of the different variables tested is shown in Figure 5. While the tissue thickness and air gap individually start to predict adjusted clay BFD, the combination of both was found to be the best predictor.

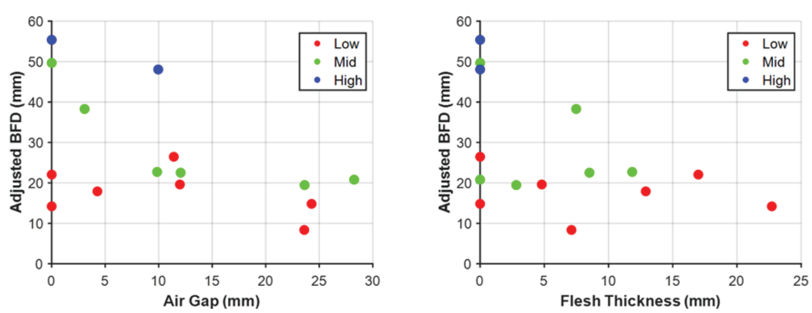

Figure 5. Adjusted clay BFD as a function of air gap (left), and tissue thickness (right) with the three striking velocities represented by the red, green and blue dots

Unlike the load cell results, the clay results were found to be best explained using a multiple linear regression to model the relationship between striking velocity, air gap, tissue thickness, and adjusted clay BFD. Utilizing the data shown in Figure 5, parameters were calculated for the linear regression model shown in equation 2. Overall, it was found that for each 1 mm of air gap or tissue thickness, there was a reduction of adjusted clay BFD values of approximately 1 mm.

$$ClayBFD(mm) = 6.295 + 0.0547 * Striking\ Vel.\left(\frac{m}{s}\right) - 1.03 * AirGap(mm) - 1.16 * TissueThick.(mm) \quad (2)$$

Table 3. Coefficients calculated for the multiple linear model fit (equation 2)

Term	Coefficient Estimate	P value
Intercept	6.295	0.2269
Striking Velocity (m/s)	0.0547	<0.0001
Air Gap (mm)	-1.03	<0.0001
Tissue Thickness (mm)	-1.16	<0.0001

3.3 PMHS outcome comparison and injury reference curve

While the models developed in equations 1 and 2 were able to accurately fit the force and clay back face deformation response respectively, investigating how this model could explain the effects of body habitus on BABT was the overall goal of this study. Using a previously collected PMHS data set, the effects of flesh thickness and air gap as it related to injury prediction was then investigated utilizing this model [2], [20]. This data set, shown in Table 4, provided 13 PMHS test data points which could be compared to the above results. From each PMHS test, the air gap, flesh thickness and striking velocity was calculated based on information collected during the test series. Similar techniques were used from the bench-top testing to collect the air gap, and the flesh thickness was measured with a pre-test CT scan at the desired anatomical impact site. Based on these values, an estimated peak primary force and adjusted clay BFD was also calculated as seen in Table 4.

Table 4. PMHS Test Matrix (Tests from Iwaskiw et al)

APL ID	Air Gap (mm)	Flesh Thickness (mm)	Striking Velocity (m/s)	Estimated Peak Primary Force (kN)	Estimated Adjusted clay BFD (mm)	Projected Operational Injury Outcome
APL01	26.0	9.1	854.35	39.53	15.69	II
APL02	12.1	10.4	756.51	84.81	23.15	II
APL03	13.2	21.5	865.33	85.19	15.09	II
APL04	12.5	15.6	657.76	54.64	11.30	I
APL05	2.9	4.5	712.62	172.34	37.07	IV
APL06	11.8	12.2	716.89	74.15	19.20	II
APL07	9.9	10.5	659.59	74.94	20.00	II
APL08	10.3	14.1	588.57	54.46	11.52	II
APL09	9.8	7.1	634.59	75.27	22.68	III
APL10	9.9	5.3	900.99	173.01	39.23	IV
APL11	10.6	18.3	917.14	130.36	24.32	IV
APL12	9.6	8.0	909.22	171.19	36.86	IV
APL13	9.2	21.1	912.57	135.55	22.26	III

As was discussed in Howes et al. 2023, a Projected Operational Injury Outcome (POIO) was calculated for each of the PMHS tested based on input from an expert panel consisting of military pathologists, trauma and general surgeons to categorise injuries based on a return to duty metric. This classification scale ranges from level I which indicates the warfighter could return to duty within 72 hours, to level IV which is thought to be a potentially fatal injury. For this study, we chose to evaluate how body habitus metrics could affect the probability of sustaining a level IV POIO as a function of striking velocity, estimated peak primary force, and estimated adjusted clay BFD. A survival analysis (SA) was applied, classifying fatal injuries as 'injured' and all other cases as 'not injured'. This approach enabled a continuous mapping of dose to injury probability, and the resulting injury curves are presented in Figure 6. The SA was unable to converge for estimated adjusted clay BFD, as some zone of mixed results (ZMR) is necessary (i.e. a dose range where, due to inherent variability, some outcomes at a given dose may result in injury while others might not). This might suggest this metric helps to differentiate between cases of non-fatal versus fatal. To evaluate the accuracy of the injury risk curves, we calculated three goodness-of-fit metrics: the Akaike Information Criterion (AIC), the Area Under the Receiver

https://doi.org/10.52202/081621-0008

Operating Characteristic Curve (AROC), and Balanced Accuracy. All three metrics improved (AIC 16.7→7.5, AROC 0.528→0.667, Balanced Accuracy 0.514→0.819) when incorporating estimated peak primary load (as derived from our fit models), indicating that injury prediction accuracy increases when body habitus is considered.

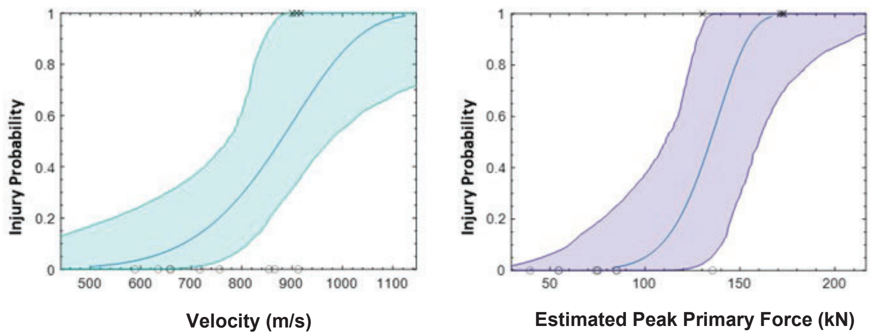

Figure 6. Probability of a fatal injury as a function of ballistic striking velocity (left) and estimated peak primary force (right)

4. DISCUSSION

To explore the effects of body habitus on BABT, this study collected data from BABT events in order to correlate loading transmitted through body armour at varying levels of air gap and flesh thickness with injury outcomes from previously conducted PMHS BABT tests. Practically, it is a challenge to collect injury data from a representative warfighter population, due to the nature and limitations of PMHS acquisition through use of specimens with great differences in age, which can be associated with body composition, to the desired population. In addition, stature, gender, and body habitus can even vary greatly across a warfighter population. There is a great utility in individually accounting for differences in body habitus and fit so that results and insights can be translated to different populations. Understanding these effects could lead to more effective standards and enable the development of more effective personal armour solutions.

4.1 Load cell response

Based on the recorded force response, we hypothesised that initial (primary) peak force correlates with injury severity. To investigate this, we examined how peak primary force varies as a function of air gap and flesh thickness. The peak forces measured in this study (17–258 kN) were greater than those observed in other blunt ballistic impact scenarios with some overlap in forces from our study's lower magnitude ballistic conditions and higher air gap and flesh thickness conditions. This may be expected due to our study's focus on ballistic velocities that induced high levels of BFD loading through a purpose-built UHMWPE plate. Bir [21] conducted tests on PMHS using law enforcement PVC batons, estimating force from impactor acceleration and mass. The values seen in that study spanned 2.6 to 4.4 kN. We observed much greater loading conditions which were likely due to the increased energy from the higher backface velocities seen in BABT [19]. Other live fire BABT testing was conducted by Bass et al on PMHS (15 kN to 30 kN) and on the AUSMAN dummy (30 kN to 70 kN) [22]. This group utilised thin profile stress gauges to obtain contact forces behind UHMWPE plates. The striking velocities in this study spanned a wider range than those in Bass et al. While force-sensing methods in BABT studies vary [23], comparing our results with previous findings highlights the role of armour fit and body habitus in force reduction. Additionally, the load magnitudes observed in this study align with simulated BABT studies where sternum loading ranges from 2.9 to 62.2 kN [24] although due to differences in the ballistic threat and soft armour modelled, direct comparisons may be inappropriate. Across all test conditions, the load cell data exhibited a bimodal peak force response, characterised by a larger initial peak followed by a lower secondary peak. This response pattern is consistent with prior ballistic force response studies [8] where the bimodal force response was observed in different ballistic testing setups and with different instrumentation packages. This bimodal response has been noted in many previous studies [22], [25]with the first peak attributed to the impedance mismatch between the armour and flesh while the second peak is associated with the local bulk motion. In these studies, the first peak was noted to have an order of magnitude more energy than the second peak. Additionally, sustained oscillations in the load cell response suggest the possible excitation of a vibrational mode within the setup. A frequency analysis of the force response identified a distinct frequency peak at approximately 8.5 kHz, well below the 30 kHz frequency limit of the PCB 200C50 load cell used in these experiments which indicates that these measurements are still valid. Overall, this study clearly showed that the air gap had a stronger correlation to peak force, both in the individual traces as well as the comparison of the overall peak response, as observed in the change of the initial peak as a function of air gap. Both air gap and flesh thickness contributed to a reduction in initial peak force, highlighting their importance in overall protection.

4.2 Clay response

Current armour systems are evaluated using clay, where maximum residual deformation is measured after ballistic impact. While challenges exist with this standard [5], no alternative has been formally established. Therefore, understanding how body habitus, specifically flesh thickness and air gap, affects clay displacement is critical. Numerous studies have used clay to assess physics-based loading parameters [6], [26] with some correlating clay BFS to kinetic energy transfer [27]. Findings from this test series indicate a strong correlation between body habitus variables and clay response, showing that each additional millimetre of offset (due to air gap or flesh thickness) reduces BFS by approximately 1 mm. If armour is typically worn with some degree of standoff from the body, performance testing standards should account for this factor. The current clay standard does not incorporate standoff, potentially representing a worst-case scenario for BABT loading. This is particularly important because armour systems optimised solely for the clay standard (without air gaps) may differ from those designed for operational wear conditions. Some designs that consider realistic air gaps and flesh thickness may offer better protection for the warfighter while minimizing weight.

4.3 Validation of body habitus effects using whole body PMHS tests

When applied to PMHS test results and injury outcomes, loading parameters adjusted for air gap and tissue thickness provided more accurate injury predictions than velocity alone. Examining the survival analysis curves in Figure 6, injury prediction models that incorporate air gap and flesh thickness show a smaller ZMR (the range where both injury and non-injury may occur) compared to those based solely on striking velocity. Additionally, when using estimated adjusted clay BFD, the potentially fatal injury group was completely separated from the non-fatal cases, suggesting that this metric effectively distinguishes injury severity. Given this complete separation, alternative binomial regression techniques could be applied for continuous injury prediction and should be considered for future analysis. These observations align with expectations, as directly measuring loading to the body and including the variations due to body habitus, should provide a stronger correlation to injury outcomes. Additionally, as was shown in equation 1, the primary peak force follows a decaying exponential function indicating that the influence of this gap diminishes as the gap increases. These results suggest that the initial few centimetres have the most critical impact on peak force which is critical for injury prediction based on the survival analysis curve and for protection. While this initial decay was best represented by an exponential fit for the load cell-based model, the clay model in equation 2 was best represented by a linear fit. Unlike the load cell-based model, the clay model appears to weight all standoff equally. Understanding the appropriate injury mechanism and injury metrics for BABT is crucial, as these two testing methods yield different conclusions regarding loading dynamics.

4.4 Limitations

While this study demonstrated strong correlations between the variables studied and injury predictions, several limitations should be considered. First, the load cell stiffness itself may have influenced the load response. The peak loads observed were higher than other studies utilizing more biofidelic surrogates. These higher forces could be attributed to armour performance (i.e. these ballistic conditions created a more severe loading condition) or due to the stiffness of the load cell system. Further testing should be done to understand the influences of the design of the backface material and armour performance on loading metrics collected. Second, although a range of PMHS specimen was used to evaluate the injury prediction, the overall sample size is small compared to the warfighter population. Since flesh thickness was found to have a protective effect, future studies should incorporate a representative range of body habitus based on the warfighter, either through additional testing or models capable of varying body composition and anthropometry. Third, while specialised fixtures were used to prepare the flesh specimens, some variance in overall thickness was expected, as is typical in PMHS testing. Further, these

https://doi.org/10.52202/081621-0008

specimens also did not include any musculature which would be expected in a living warfighter population. Lastly, this study presents air gap and flesh thickness as a single value for each impact test, where likely these values vary over the impact site. Converting these simple one-dimensional metrics to three-dimensional values may better explain these parameter effects on loading, especially when considering body regions with more spatial variance of body shape and body tissue composition. However, the contact area for this loading event is small, and the spatially varying air gap and flesh thickness may vary less than in the contact region in more broadly distributed loading events. These limitations warrant further investigation in the effect of body habitus on BABT injury response.

5. CONCLUSION

This study demonstrated that body habitus, as described by varying levels of air gap and flesh thickness, was highly correlated to the BABT loading, as measured using load cell and clay backed methods. Additionally, incorporating these body habitus parameters improved injury outcome predictions in previously conducted PMHS BABT tests. Specifically, increased air gap and flesh thickness were associated with lower measured and predicted force responses, suggesting that these factors play a critical role in reducing injury risk. These results are essential for developing more effective standards and more effective personal armour solutions.

Acknowledgments

The authors would like to express their appreciation to the U.S. Special Operations Command for funding this work under Contract No. H92236-10-D-001, Task Order 0521.

References

[1] A. W. Carroll and C. A. Sonderstrom, “"A new nonpenetrating ballistic injury,” *Annals of Surgery,* vol. 188, no. 6, p. 753, 1978.

[2] A. Iwaskiw, et al., “Initial injury observations in postmortem human subjects: Non-penetrating ballistic impacts over the sternum with lightweight hard armour plates,” in *Personal Armour System Symposium*, Copenhagen, Denmark, 2021.

[3] T. Talmy, et al., “"Close-range fire inflicting behind armor blunt trauma: case-series and implications for battlefield care,” *Military Medicine,* vol. 189, no. 1-2, pp. e448-e453, 2024.

[4] US Department of Justice, “Ballistic resistance of police body armor NIJ Standard-0101.07.2024,” *National Institute of Justice - Office of Law Enforcement Standards,* pp. 1-13, 1986.

[5] National Research Council, “Testing of body armor materials: Phase III,” *National Academies Press,* 2012.

[6] M. Eaton, et al., “Testing the validity of the NIJ clay standard for approving body armor with a preliminary insight into injury correlation,” *ASME International Mechanical Engineering Congress and Exposition,* 2020.

[7] C. R. Bass, “Helmet behind armor blunt trauma,” in *Specialist Conference on Human Factors in Medicine*, Koblenz, Germany, 2003.

[8] A. Iwaskiw and et al, “Loads Associated with Behind Helmet Blunt Trauma: Matched-Pair Load Sensing Headform Tests Correlated with Skull Fracture Severity,” in *Personal Armour Systems Symposium*, Dresden, Germany, 2023.

[9] J. McMahon, et al., “Development of Impulse-Based Rib Fracture Injury Criterion for Behind Armor Blunt Trauma,” in *IRCOBI Conference*, 2023.

[10] J. McMahon, et al., “Use of a Porcine Cadaver Model as a Human Surrogate for Behind Armor Blunt Trauma,” *Journal of Engineering and Science in Medical Diagnostics and Therapy,* vol. 8.4, 2025.

[11] R. Kraft, et al., “Modeling Skeletal Injuries in Military Scenarios,” *The Mechanobiology and Mechanophysiology of Military- Related Injuries,* pp. 3-35, 2016.

[12] Kim and Han, “Virtual fit assessment of US army body armor using NASA spacesuit techniques,” *Applied Ergonomics 120,* vol. 104339, 2024.

[13] M. Reed and D. William, “Creating human figure models for ergonomic analysis from whole-body scan data,” *Proceedings of the Human Factors and Ergonomics Society Annual Meeting,* vol. 45, 2001.

[14] S. Moran, et al., “Injury rates among restrained drivers in motor vehicle collisions: the role of body habitus,” *Journal of Trauma and Acute Care Surgery,* pp. 1116-1120, 2002.

[15] S. Wang, et al., “Increased depth of subcutaneous fat is protective against abdominal injuries in motor vehicle collisions,” *Annual Proceedings/Association for the Advancement of Automotive Medicine,* vol. 47, 2003.

[16] J. Choi, et al., “Body mass index and mortality in blunt trauma: the right BMI can be protective,” *The American Journal of Surgery,* vol. 220, no. 6, pp. 1475-1479, 2020.

[17] S. Dogruyol and T. Dogruyol, “Adipose tissue provides a cushioning effect in low-energy isolated blunt thoracic trauma: a prospective observational,” *Acta Chir Belg,* vol. 123, no. 4, pp. 396-404, 2023.

[18] D. Hisley, J. Gurganus and A. Drysdale, “Experimental Methodology Using Digital Image Correlation to Assess Ballistic Helmet Blunt Trauma,” *J Appl Mech,* vol. 78, no. 5, p. 051022, 2011.

[19] Y. K. Wen, “Analysis of dynamic back face deformation of a body armor impact by a rifle bullet using 3D-DIC,” *Journal of Physics: Conference Series,* vol. 1507, no. 5, 2020.

[20] C. Howes, et al., “Injuries and Operational Implications Caused By Behind Armour Blunt Trauma Across Various Impact Locations,” in *Personal Armour Systems Symposium*, Dresden, Germany, 2023.

[21] C. Bir, D. Viano and A. King, “Development of biomechanical response corridors of the thorax to blunt ballistic impacts,” *Journal of Biomechanics,* vol. 37, no. 1, pp. 73-79, 2004.

[22] C. Bass and et al, “Injury Risk in behind armor blunt thoracic trauma,” *International Journal of Occupational Safety and Ergonomics,* vol. 12, no. 4, pp. 429-442, 2006.

[23] B. Anctil, et al., “Evaluation of impact force measurement systems for assessing behind armour blunt trauma for undefeated ballistic helmets,” in *Personal Armour Systems Symposium,*, The Hague, The Netherlands, 2004.

[24] M. C. Bustamante and D. S. Cronin, “Impact location dependence of behind armor blunt trauma injury assessed using a human body finite element model,” *Journal of biomechanical engineering,* vol. 146, no. 3, 2024.

[25] J. van Bree and P. Gotts, “The "twin peaks" of BABT,” in *Proceeding from the 5th Personal Armour Systems Symposium*, Clochester, UK, 2000.

[26] D. Bhattacharjee, A. Kumar and B. Ipsita, “Energy absorption and dynamic deformation of backing material for ballistic evaluation of body armour,” *Defence Science Journal,* vol. 63, no. 5, pp. 462-466, 2013.

[27] M. Bevan, et al., “Correlation between Round Kinetic Energy and Displaced Clay Volume for Three Classes of Armour,” in *Personal Armour Systems Symposium*, Washington DC, USA, 2018.

 https://doi.org/10.52202/081621-0008